Exchange interactions in III-V and group-IV diluted magnetic semiconductors

J. Kudrnovský,[1,4,5] I. Turek,[2,3,4] V. Drchal,[1,4] F. Máca,[1,4] P. Weinberger,[4] and P. Bruno[5]
[1]*Institute of Physics, Academy of Sciences of the Czech Republic, Na Slovance 2, CZ-182 21 Prague 8, Czech Republic*
[2]*Institute of Physics of Materials, Academy of Sciences of the Czech Republic, Žižkova 22, CZ-616 62 Brno, Czech Republic*
[3]*Department of Electronic Structures, Charles University, Ke Karlovu 5, CZ-121 16 Prague 2, Czech Republic*
[4]*Center for Computational Materials Science, Technical University of Vienna, Getreidemarkt 9, A-1060 Vienna, Austria*
[5]*Max-Planck Institut für Mikrostrukturphysik, Weinberg 2, D-06120 Halle, Germany*
(Received 26 March 2002; revised manuscript received 7 November 2003; published 17 March 2004)

Effective pair exchange interactions between Mn atoms in III-V and group-IV diluted magnetic semiconductors are determined from a two-step first-principles procedure. In the first step, the self-consistent electronic structure of a system is calculated for a collinear spin structure at zero temperature with the substitutional disorder treated within the framework of the coherent-potential approximation. The effective exchange pair interactions are then obtained in a second step by mapping the total energies associated with rotations of magnetic moments onto an effective classical Heisenberg Hamiltonian using the magnetic force theorem and one-electron Green functions. The formalism is applied to $Ga_{1-x}Mn_xAs$ alloys with and without As antisites, and to $Ge_{1-x}Mn_x$ alloys recently studied experimentally. A detailed study of the behavior of pair exchange interactions as a function of the distance between magnetic atoms as well as a function of the concentrations of the magnetic atoms and compensating defects is presented. We have found that due to disorder and the half-metallic character of the system the pair exchange interactions are exponentially damped with increasing distance between the Mn atoms. The exchange interactions between Mn atoms are ferromagnetic for distances larger than the ones corresponding to the averaged nearest-neighbor Mn-Mn distance. The pair exchange interactions are also reduced with increasing concentrations of the Mn atoms and As antisites. As a simple application of the calculated exchange interactions we present mean-field estimates of Curie temperatures.

DOI: 10.1103/PhysRevB.69.115208 PACS number(s): 75.50.Pp, 71.15.Nc, 71.20.Nr, 75.30.Et

I. INTRODUCTION

The diluted III-V magnetic semiconductors (DMS) are materials which exhibit spontaneous ferromagnetism mediated by holes in the valence band of the host semiconductor and thus represent new materials with promising applications in spintronics. They have attracted a great deal of attention from both the experimental[1] and theoretical[2,3] points of view. Most of the effort in the past has focused on III-V compounds but theoretical investigations based on the mean-field solution of the so-called kinetic exchange model[2] (KEM) have predicted also ferromagnetism in group-IV semiconductors.[3] Recently such compounds were prepared by two groups[4,5] with a Curie temperature of the same order as in III-V compounds.

In this paper we present a systematic first-principles study of pair exchange interactions in (Ga,Mn)As and (Ge,Mn) DMS as a function of both the distance between magnetic atoms and the impurity concentrations. The knowledge of these exchange interactions allows one to address in detail the character of magnetic excitations in the DMS. Magnetic excitations in ferromagnets are of two different kinds, namely, Stoner excitations associated with longitudinal fluctuations of the magnetization, and spin waves, or magnons corresponding to collective transverse fluctuations of the magnetization direction. The low-temperature regime is dominated by magnons, and Stoner excitations can be neglected. Pair exchange interactions thus allow one to evaluate the Curie temperature, the spin-wave stiffness, and the spectrum of low-lying magnetic excitations.

We shall adopt here a two-step procedure[6] which consists in mapping of the complicated itinerant electron system onto an effective Heisenberg Hamiltonian and a consequent application of statistical mechanical methods. The validity of this approach, based on the adiabatic approximation, is in particular justified for magnetic atoms with large exchange splittings, such as, e.g., Mn atoms. The mapping is further simplified by using the magnetic force theorem[6] which states that the band energy of the calculated ground state with a collinear spin structure can be used as an estimate for corresponding total-energy differences. Recently, we have calculated first-principles effective pair exchange interactions in real space for bulk transition metals,[7] rare-earth metals,[8] as well as for low-dimensional systems such as ultrathin films,[9] and used these interactions in order to estimate Curie temperatures and magnon spectra, which were in a good agreement with the available experimental data. Here we extend this approach to a random system, in particular to the DMS.

Ground-state density-functional calculations of DMS, which form the first step for a mapping to a Heisenberg model, fall into two groups. One group consists of a supercell approaches[10–14] in which big cells are used to describe low concentrations of magnetic atoms and other impurities. In the other group Green-function methods are employed in which the configurational averaging is performed within the coherent-potential approximation (CPA) as implemented, e.g., in terms of the Korringa-Kohn-Rostoker method[15–18] or the tight-binding linear muffin-tin orbital method (TB-LMTO). Both groups have advantages and drawbacks. The CPA, e.g., can treat any alloy composition whereas proper description of very low concentrations of various impurities typical for DMS in the framework of the supercell approach

is numerically quite demanding. The CPA also takes properly into account effects of finite lifetimes of electronic states caused by disorder, which are neglected in a supercell approach. On the other hand, the CPA does not include local environment effects which to some extent can be simulated by a supercell approach. The mapping of calculated ground states to a Heisenberg model and a determination of pair exchange interactions between magnetic atoms, however, can be also performed on the basis of supercell calculations.[4,19]

II. FORMALISM

Here we briefly summarize the computational details and the direct evaluation of the effective pair exchange interactions.

A. Electronic structure

We have determined the electronic structure of the DMS in the framework of the first-principles all-electron TB-LMTO method in the atomic-sphere approximation[20] using empty spheres in the interstitial tetrahedral positions of the zinc-blende or diamond lattice needed for a good space filling. We used equal Wigner-Seitz radii for all sites. The valence basis consists of *s*, *p*, and *d* orbitals; we included scalar-relativistic corrections but neglected spin-orbit effects. Substitutional disorder due to various impurities, both magnetic and nonmagnetic, is included by means of the CPA. Charge self-consistency is treated within the framework of the local spin-density approximation using the Vosko-Wilk-Nusair parametrization for the exchange-correlation potential.[21] The experimental lattice constants of the host semiconductor, $a=5.653$ Å for GaAs and $a=5.658$ Å for Ge, were used also for $(Ga_{1-x-y}Mn_xAs_y)As$ and $Ge_{1-x}Mn_x$ alloys. We have verified, however, that we can neglect a weak dependence of the sample volume on defect concentrations. Further details of the method can be found in Ref. 22.

B. Effective pair exchange interactions

We now briefly describe the mapping of the total energy of a spin-polarized electron system onto an effective classical Heisenberg model[6,7]

$$H=-\sum_{i\neq j} J_{ij}\mathbf{e}_i\cdot\mathbf{e}_j\,. \tag{1}$$

Here, $\mathbf{e}_i$ and $\mathbf{e}_j$ are the unit vectors of the local magnetic moments at sites i and j, and the J_{ij} denote the effective pair exchange interactions between atoms carrying magnetic moments. It should be noted that in the present formulation the values and signs of the magnetic moments are already absorbed in the definition of the J_{ij}'s: positive (negative) values correspond to ferromagnetic (antiferromagnetic) coupling.

For applications to the DMS, we have to generalize the theoretical approach developed in Refs. 6 and 7 to disordered systems. The Heisenberg parameters are obtained in terms of the magnetic force theorem[6] by (i) directly evaluating the change in energy associated with a small rotation of the spin-polarization axes in atomic cells i and j, and (ii) using the vertex-cancellation theorem (VCT).[23,24] The VCT justifies the neglect of disorder-induced vertex corrections in Eq. (2) and greatly simplifies calculations. The VCT was derived in Ref. 24 under rather general conditions and it facilitates an efficient evaluation of exchange interactions, exchange stiffnesses, spin-wave energies, etc. The derivation of configurationally averaged effective pair exchange interactions $\overline{J}_{ij}^{M,M'}$ between two magnetic atoms M,M' located at sites i and j follows therefore closely the case without randomness:[6,7]

$$\overline{J}_{ij}^{M,M'}=\frac{1}{4\pi}\mathrm{Im}\int_C \mathrm{tr}_L[\,\delta_i^M(z)\overline{g}_{ij}^{M,M'\uparrow}(z)\,\delta_j^{M'}(z)\overline{g}_{ji}^{M',M\downarrow}(z)\,]dz\,. \tag{2}$$

Here, tr_L denotes the trace over angular momenta $L=(\ell m)$, the energy integration is performed in the upper half of the complex energy plane along a contour C starting below the bottom of the valence band and ending at the Fermi energy, and $\delta_i^M(z)=P_i^{M,\uparrow}(z)-P_i^{M,\downarrow}(z)$, where the $P_i^{M,\sigma}(z)$ are the L-diagonal matrices of potential functions for $\sigma=\uparrow,\downarrow$ corresponding to a particular magnetic atom M. The matrix $\delta_i^M(z)$ reflects the exchange splitting of atom M. The quantities $\overline{g^{M,M'\uparrow}}_{ij}(z)$ and $\overline{g^{M',M\downarrow}}_{ji}(z)$ refer to site off-diagonal blocks of the conditionally averaged Green function,[22] namely, the average of the Green function over all configurations with atoms of the types M and M' fixed at sites i and j, respectively. The exchange interactions between magnetic moments induced on nonmagnetic atoms are negligible as compared to the exchange interactions between substitutional Mn atoms on the Ga sublattice or on two equivalent Ge sublattices, i.e., $M=M'=\mathrm{Mn}$. The main advantage of the present approach is an explicit expression for $\overline{J}_{ij}^{\mathrm{Mn,Mn}}$ which can be evaluated straightforwardly even for large distances $d=|\mathbf{R}_i-\mathbf{R}_j|$ between sites i and j and thus allows us to study their asymptotic behavior as a function of the distance d. The effect of impurities on the host band structure, which need not be a small perturbation, is usually neglected in model theories,[2,3] where the unperturbed host Green function appears in Eq. (2) rather than its conditionally averaged counterpart $\overline{g^{\mathrm{Mn,Mn}\sigma}}_{ij}(z)$.

In the low-concentration limit Eq. (2) reproduces correctly the Ruderman-Kittel-Kasua-Yosida (RKKY) type expression for exchange interactions between two magnetic impurities in a nonmagnetic host:[25]

$$J_{ij}^{\mathrm{RKKY}}=\frac{1}{4\pi}\mathrm{Im}\int_C \mathrm{tr}_L\{\delta_i^{\mathrm{imp}}(z)g_{ij}^{\mathrm{imp},\uparrow}(z)\,\delta_j^{\mathrm{imp}}(z)g_{ji}^{\mathrm{imp},\downarrow}(z)\}dz\,. \tag{3}$$

Here, $g_{ij}^{\mathrm{imp},\sigma}(z)$ is the Green function of two Mn impurities embedded in the semiconductor host, evaluated at sites i,j where impurities are located. A conventional RKKY expression is obtained by replacing the spin-dependent impurity Green function $g_{ij}^{\mathrm{imp},\sigma}(z)$ by the nonmagnetic ideal Green function $g_{ij}^{\mathrm{GaAs}}(z)$ or $g_{ij}^{\mathrm{Ge}}(z)$ of the host crystal. The neglect of the renormalization of the host Green function by scatterings on impurities is twofold: it introduces a phase factor and

modifies the amplitude of the oscillations as compared to the conventional RKKY formula.[25]

It should be noted that the numerical evaluation of expressions (2) and (3), in particular for large distances, requires a careful Brillouin-zone (BZ) integration (typically, 10^5–10^6 of **k** points in the full BZ are needed for large distances such as 10 lattice constants and more, and for energy points on the contour C close to the Fermi energy). The exchange interactions in real space can be evaluated also in the frozen magnon approach applied in supercell schemes by means of an inverse Fourier transformation. The calculated values of $\overline{J}_{ij}^{M,M'}$ are, however, limited to a subset of all possible pairs of magnetic atoms which in turn form an ordered subset of magnetic sites on the lattice.[19]

C. Curie temperatures

Once the effective pair exchange interactions are determined a number of relevant quantities related to the magnetic state can be determined. In particular, the mean-field value (MFA) of the Curie temperature (T_c) is simply given by

$$k_B T_c^{\mathrm{MFA}} = \frac{2x}{3} \sum_{i(i\neq 0)} \overline{J}_{0i}^{\mathrm{Mn,Mn}}, \tag{4}$$

where the sum extends over all sites occupied by Mn atoms on the Ga sublattice or on two equivalent Ge sublattices for $(Ga_{1-x}Mn_x)As$ and $Ge_{1-x}Mn_x$ alloys, respectively.

The simplest way of estimating T_c is an evaluation of the effective on-site exchange parameter for Mn atom J_i^{Mn} defined as[6,7]

$$\overline{J}_i^{\mathrm{Mn}} = -\frac{1}{4\pi}\mathrm{Im}\int_C \mathrm{tr}_L\{\delta_i^{\mathrm{Mn}}(z)[\overline{g}_{ii}^{\mathrm{Mn},\uparrow}(z) - \overline{g}_{ii}^{\mathrm{Mn},\downarrow}(z)] + \delta_i^{\mathrm{Mn}}(z)\overline{g}_{ii}^{\mathrm{Mn},\uparrow}(z)\,\delta_i^{\mathrm{Mn}}(z)\overline{g}_{ii}^{\mathrm{Mn},\downarrow}(z)\}dz. \tag{5}$$

In Eq. (5) the quantities $\overline{g}_{ii}^{\mathrm{Mn},\sigma}(z)$ ($\sigma=\uparrow,\downarrow$) refer to the site-diagonal blocks of the conditionally averaged Green function, namely, to the average of the Green function over all configurations with a Mn atom fixed at the site i.[22] The mean-field value of T_c is then simply given by

$$k_B T_c^{\mathrm{MFA}} = \tfrac{2}{3}\overline{J}_i^{\mathrm{Mn}}. \tag{6}$$

The effective on-site exchange parameter $\overline{J}_i^{\mathrm{Mn}}$ has the physical meaning of an exchange field produced by all neighboring magnetic moments acting on the Mn atom at the site i (Ref. 6),

$$\overline{J}_i^{\mathrm{Mn}} = x \sum_{j(j\neq i)} \overline{J}_{ij}^{\mathrm{Mn,Mn}}. \tag{7}$$

The mean-field expressions for T_c, Eqs. (6) and (4), are in principle mutually equivalent. Expression (6) has some advantages as compared to Eq. (4): it does not require a summation over all shells and includes contributions from small induced moments on nonmagnetic atoms. On the other hand, expression (4) can be generalized to alloys with few different magnetic atoms. It should be noted that recent studies[26,27] confirm that the mean-field approximation estimate of T_c in DMS is well justified.

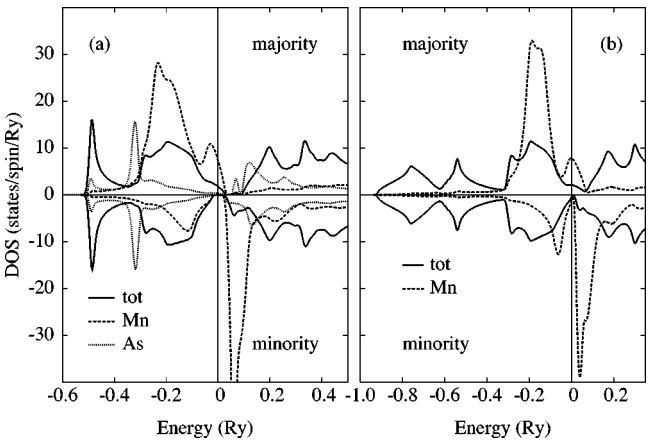

FIG. 1. Spin-dependent total densities of states and local Mn densities of states for (a) ferromagnetic $(Ga_{0.94}Mn_{0.05}As_{0.01})As$ and (b) ferromagnetic $Ge_{0.975}Mn_{0.025}$ alloys. The Fermi level coincides with the energy zero.

For a matter of completeness, we mention another simple estimate of T_c as obtained from first-principles calculations by relating T_c to the total energy difference Δ per unit cell between the ferromagnetic and the disorder local moment (DLM) state,[28,29] i.e., $\Delta = E_{\mathrm{DLM}} - E_{\mathrm{FM}}$,

$$k_B \tilde{T}_c = 2\Delta/3x. \tag{8}$$

Results based on Eqs. (8) and (4) agree reasonably well with each other;[28] Eq. (8), however, cannot be generalized to alloys containing more than one kind of magnetic atoms with different concentrations.

III. RESULTS

We have calculated the exchange interactions $\overline{J}_{ij}^{\mathrm{Mn,Mn}}$ as a function of the interatomic distance $d=|\mathbf{R}_i-\mathbf{R}_j|$ and studied the effect of impurities in ferromagnetic $(Ga_{1-x-y}Mn_xAs_y)As$ and $Ge_{1-x}Mn_x$. As a simple illustration of the calculated exchange interactions we present mean-field estimates of the Curie temperature.

A. Electronic properties

In Fig. 1 calculated total densities of states (DOS) as well as local DOS for the Mn atoms in $(Ga_{0.94}Mn_{0.05}As_{0.01})As$ and $Ge_{0.975}Mn_{0.025}$ alloys are shown. The results for (Ga, Mn)As alloys, Fig. 1(a), are in a good agreement with both supercell and CPA studies for alloys without As antisites.[12,13,19,29] The main effect of As antisites on the DOS is a shift of the Fermi level toward the top of the valence band thus reducing the number of hole carriers in comparison with the case without As antisites, and the presence of localized states due to As antisites in the gap of the majority states (see also Ref. 18). The results for (Ge,Mn) alloys, Fig. 1(b), are similar to those for (Ga,Mn)As alloys: there is a well pronounced Mn peak in the local Mn-DOS inside the

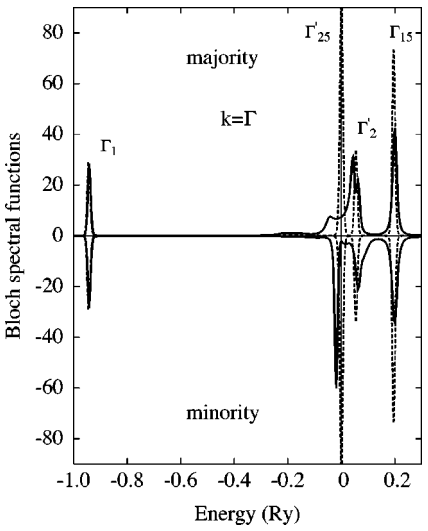

FIG. 2. Spin-dependent Bloch spectral functions at the Γ point corresponding to the Ge sublattices for ferromagnetic $Ge_{0.975}Mn_{0.025}$ (full lines) and for a reference pure Ge system (dashed lines).

valence band and there are Mn-induced states at the top of the valence band in which the Fermi level lies. The width of the Mn-local DOS is larger for (Ga,Mn)As thus indicating a stronger *pd* hybridization as compared to (Ge,Mn) alloys. Another important feature observed in both alloy systems is their half-metallic character: the Fermi level lies in the gap of the minority states but inside the valence band. The half-metallic character has two important consequences: (i) an integer value of the total magnetic moment per Mn atom, namely, 4 μ_B and 3 μ_B for (Ga,Mn)As and (Ge,Mn) alloys, respectively; and (ii) it leads to an exponential damping of exchange interactions between the Mn atoms with distance (see Sec. III B). The calculated total magnetic moments per Mn atom are in a good agreement with other theoretical studies[12,13,19,29] and with experiments for (Ge,Mn) alloys.[4] The calculated DOS indicate that the majority and minority states are influenced differently by disorder: while the majority DOS differs non-negligibly from the corresponding host semiconductor DOS, the minority DOS closely resembles it. The most detailed description of the influence of disorder on electronic states is provided by Bloch spectral functions (BSF), which in random alloys substitute the concept of electron bands.[22] We illustrate this point for the BSF calculated at the Γ point ($\mathbf{k}=\mathbf{0}$) in the case of $Ge_{0.975}Mn_{0.025}$, Fig. 2. We show there in dashed lines the BSF's of the pure Ge host which are simply δ-function-like at energies corresponding to the electronic bands at $\mathbf{k}=\mathbf{0}$. As can be seen in the energy region of the Mn states, $E \in (-0.2,0.1)$ Ry, the valence minority states are only very weakly broadened by disorder and exhibit quasiparticle behavior, while both the valence (Γ'_{25}) and the conduction (Γ'_2) majority states are strongly influenced by disorder and no longer exhibit quasiparticle behavior. It is obvious that the effect of disorder is important close to the Fermi energy and does modify the values of $\overline{J}_{ij}^{\mathrm{Mn,Mn}}$, Eq. (2). In particular, the damping of electronic states as illustrated in Fig. 2 leads to a damping of the $\overline{J}_{ij}^{\mathrm{Mn,Mn}}$ with increasing distance between Mn atoms (see Sec. III B).

B. Exchange interactions: theoretical remarks

We will first discuss qualitatively the dependence of $\overline{J}_{ij}^{\mathrm{Mn,Mn}}$ on the distance $R_{ij}=|\mathbf{R_i}-\mathbf{R_j}|$. In the limit of large values of R_{ij} the expression (2) can be evaluated analytically by means of the stationary phase approximation.[7] By generalizing the approach developed in Ref. 7, we obtain

$$\overline{J}_{ij}^{\mathrm{Mn,Mn}} \propto \exp(-\boldsymbol{\lambda}_{ij}^{\uparrow}\cdot\mathbf{R}_{ij}) \times \exp(-\boldsymbol{\kappa}_{\mathrm{F}}^{\downarrow}\cdot\mathbf{R}_{ij})\frac{\sin(\mathbf{k}_{\mathrm{F}}^{\uparrow}\cdot\mathbf{R}_{ij}+\Phi^{\uparrow}+\Phi^{\downarrow})}{R_{ij}^{3}}. \quad (9)$$

The quantity $\mathbf{k}_{\mathrm{F}}^{\sigma}$, which characterizes the period of oscillations, is the Fermi wave vector in a direction such that the associated group velocity $\nabla_{\mathbf{k}}\overline{E}^{\sigma}(\mathbf{k}_{\mathrm{F}})$ is parallel to $\mathbf{R}_{ij}$. Because of disorder, the band energy $\overline{E}^{\sigma}(\mathbf{k})$ is modified by the real part of the corresponding spin-dependent self-energy at the Fermi energy (determined within the CPA) while its imaginary part characterizes the damping $\boldsymbol{\lambda}_{ij}^{\sigma}$. The damping due to disorder is anisotropic inside the BZ,[22] the factor $\boldsymbol{\lambda}_{ij}^{\uparrow}$ therefore depends on the direction of $\mathbf{R}_{ij}$. Because of the half-metallic character of (Ga,Mn)As and (Ge,Mn) alloys (a fully occupied minority band), the corresponding critical Fermi wave vector $\mathbf{k}_{\mathrm{F}}^{\downarrow}$ of the minority states is complex, $\boldsymbol{\kappa}_{\mathrm{F}}^{\downarrow} = \mathrm{Im}\mathbf{k}_{\mathrm{F}}^{\downarrow}$. This situation is similar to that studied in Ref. 7 for strong ferromagnets with a fully occupied majority band. Finally, $\Phi^{\uparrow}$ and $\Phi^{\downarrow}$ denote the corresponding phase factors. For the alloy case we thus find an exponential damping of $\overline{J}^{\mathrm{Mn,Mn}}$ with the distance, because of (i) the damping due to substitutional disorder which was predicted by de Gennes,[30] and (ii) additional damping due to the half-metallic character of (Ga,Mn)As and (Ge,Mn) alloys. It should be noted that both types of damping are missing in simple model theories that assume an unperturbed host semiconductor.[2] The damping due to disorder refers to configurationally averaged exchange interactions whereby exchange interactions in each alloy configuration can exhibit a slower decay with a distance.[31] The averaged exchange interactions are sampled directly or indirectly in experiments when measuring, e.g., Curie temperatures and spin-wave spectra.

C. Exchange interactions: $(Ga_{1-x-y}Mn_xAs_y)As$

The dependence of the exchange interactions $\overline{J}_{ij}^{\mathrm{Mn,Mn}}$ on the distance between Mn impurities for disordered $(Ga_{0.95}Mn_{0.05})As$ and for a model of two Mn impurities in an ideal GaAs host [Eq. (3)] with the Fermi level shifted into the valence band to accommodate the same number of valence holes as for $(Ga_{0.95}Mn_{0.05})As$ is shown in Fig. 3. We have calculated values of $\overline{J}^{\mathrm{Mn,Mn}}(d)$ corresponding to more than 200 coordination shells in the disordered fcc-Ga sublattice to verify the asymptotic behavior. The expected decay of the exchange interactions with distance is clearly seen in both cases [Fig. 3(a)]; for a quantitative analysis, however, we need a different presentation of results. A suitable way, e.g., is to plot $\ln|d^3\overline{J}^{\mathrm{Mn,Mn}}(d)|$ as a function of the distance d. From such a presentation one can extract straightforwardly

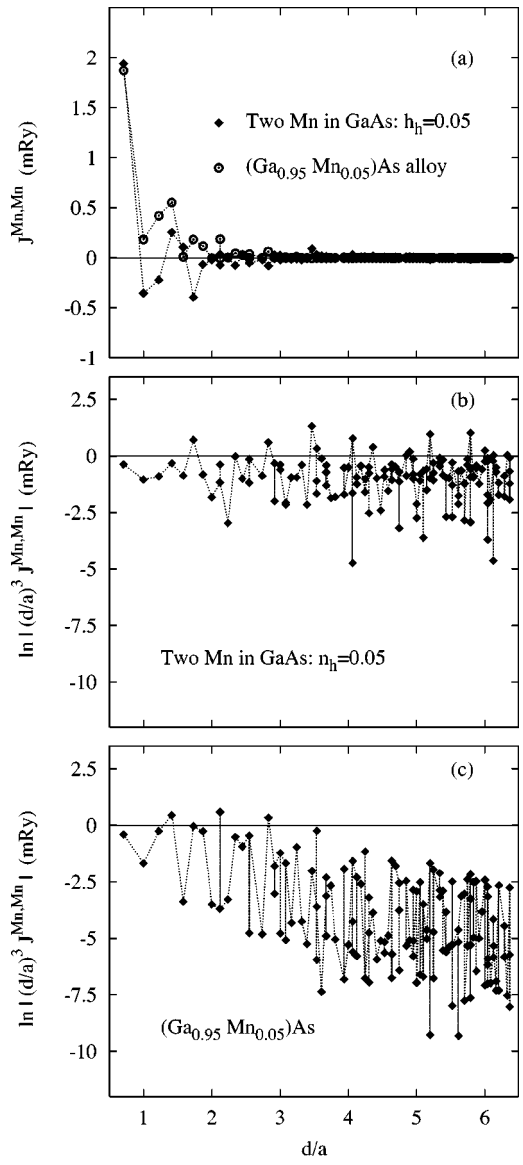

FIG. 3. (a) Dependence of $\overline{J}^{\mathrm{Mn,Mn}}(d/a)$ on the distance d in ferromagnetic $(Ga_{0.95}Mn_{0.05})As$ and, for two Mn impurities, in GaAs with the same number of valence holes $n_h=0.05$; (b,c) dependence of $\ln|(d/a)^3\overline{J}^{\mathrm{Mn,Mn}}(d/a)|$ on the distance d for above two cases.

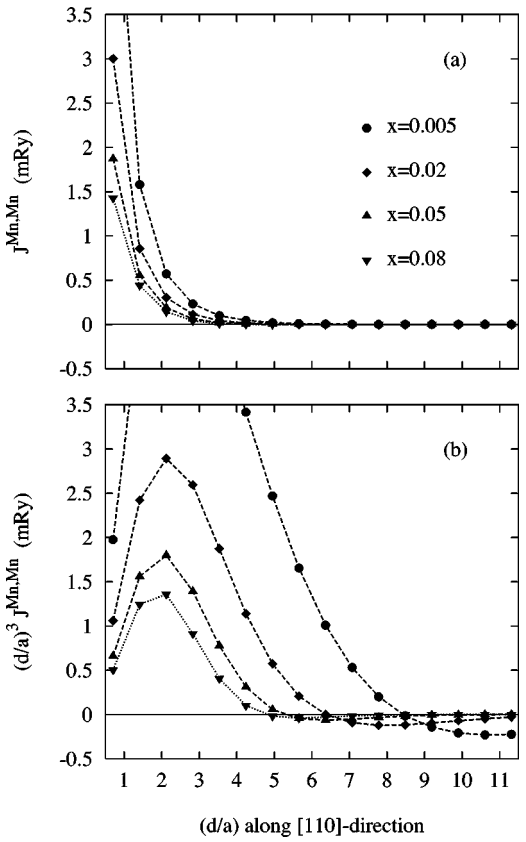

FIG. 4. Dependence of pair exchange interactions on the distance d between two Mn atoms along the nearest-neighbor direction [110] in ferromagnetic $(Ga_{1-x}Mn_x)As$ for four different concentrations x: (a) $\overline{J}^{\mathrm{Mn,Mn}}(d/a)$ and (b) $(d/a)^3\overline{J}^{\mathrm{Mn,Mn}}(d/a)$.

the expected exponential damping [see Figs. 3(b) and 3(c)]. For the model of two impurities we observe essentially a RKKY-type behavior without damping. For the alloy case, on the contrary, we find a well-pronounced exponential damping of $\overline{J}^{\mathrm{Mn,Mn}}(d)$ with distance. It should be noted that the exchange interactions are strongly anisotropic with respect to different directions $\mathbf{d}=\mathbf{R}_i-\mathbf{R}_j$. A more detailed study of $\overline{J}^{\mathrm{Mn,Mn}}(d)$ as calculated along the (dominating) nearest-neighbor direction [110] on the Ga sublattice is presented in Figs. 4 and 5. We observe exponentially damped oscillations for $(Ga_{0.95}Mn_{0.05})As$ (Fig. 4) with a period of about $5.5a$, where a is the lattice constant. This period is larger than the average distance $\overline{d}^{\mathrm{Mn,Mn}}$ between two Mn nearest neighbors at a given concentration x. A simple estimate for $\overline{d}^{\mathrm{Mn,Mn}}$ is given by

$$\overline{d}^{\mathrm{Mn,Mn}}=2\sqrt[3]{\frac{3}{B\pi x}}a, \tag{10}$$

where $B=16$, 32 for (Ga,Mn)As and (Ge,Mn) alloys, respectively. For $(Ga_{0.95}Mn_{0.05})As$ this estimate yields $\overline{d}^{\mathrm{Mn,Mn}}=2.12a$.

The leading exchange interactions $\overline{J}^{\mathrm{Mn,Mn}}(d)$ in $(Ga_{0.95}Mn_{0.05})As$, Fig. 4(a), are essentially ferromagnetic, and, because of the damping, the antiferromagnetic values are very small due to a large oscillation period. This finding supports the basic assumption made in model studies: the coupling between two Mn atoms is ferromagnetic and oscillatory with a period that exceeds the typical interatomic distance between magnetic atoms because of the small size of the corresponding hole Fermi surface. This feature is clearly illustrated in Fig. 4(b) where we plot $(d/a)^3\overline{J}^{\mathrm{Mn,Mn}}(d)$ as a function of the distance between two Mn atoms: the smaller the concentration x, i.e., the smaller the size of the corresponding hole Fermi surface, the larger the period of the damped oscillations. It should be noted that next nearest-neighbor interactions are important and contribute significantly to the value of T_c [see Eq. (4)]. For example, the first

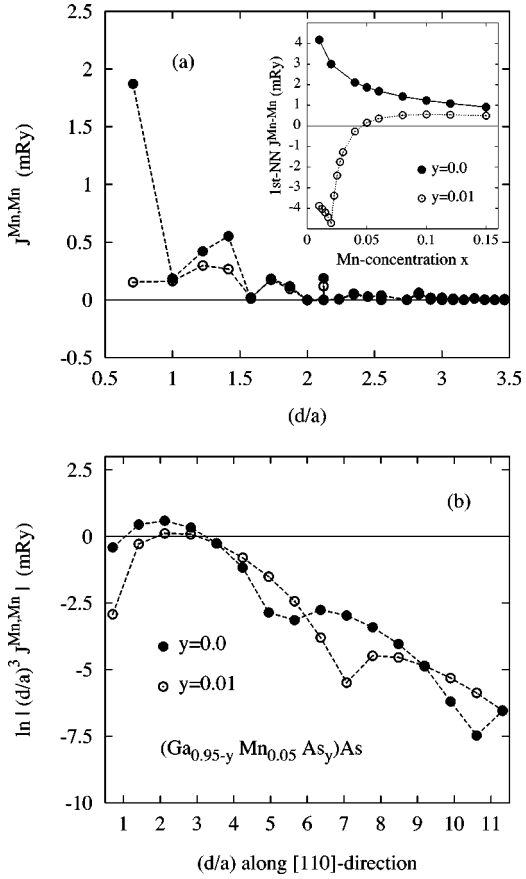

FIG. 5. Exchange interactions in ferromagnetic $(Ga_{0.95-y}Mn_{0.05}As_y)As$ for two different concentrations y of As antisites: (a) $\bar{J}^{Mn,Mn}(d/a)$ as a function of the distance d between two Mn atoms. In the inset the first nearest-neighbor exchange interactions $\bar{J}_1^{Mn,Mn}$ are shown as a function of the Mn concentration x; (b) $\ln|(d/a)^3\bar{J}^{Mn,Mn}(d/a)|$ as a function of the distance d between two Mn atoms along the nearest-neighbor direction [110].

two (four) nearest-neighbor shells contribute about 50% (75%) to the value of T_c [see Fig. 4(a)].

The effect of As antisites on the Ga sublattice on exchange interactions is illustrated in Fig. 5, where we compare the results for $(Ga_{0.95-y}Mn_{0.05}As_y)As$ with $y=0$ and $y=0.01$. As can be seen from Fig. 5(b) for the case of the [110] direction, the presence of As antisites reduces the number of holes in the valence band which in turn leads to an enlarged period of damped oscillations for $y=0.01$. It should be noted that the oscillations for both $y=0$ and $y=0.01$ are exponentially damped, the damping being slightly larger in the case with As antisites. The first nearest-neighbor interactions are reduced by nearly an order of magnitude as compared to the case without antisites while the reduction of other interactions is less pronounced [see Fig. 5(a)].

The dependence of the exchange interactions between the first nearest neighbors as a function of the Mn concentration with and without the doping by As antisites is shown in the inset of Fig. 5(a). In general, we observe a decrease of the leading $\bar{J}_1^{Mn,Mn}$ with increasing concentrations of both Mn atoms and As defects, the decrease with increasing concentration y of As antisites being weaker. The $\bar{J}_1^{Mn,Mn}$ are ferromagnetic in alloys without donors, but may change their sign for highly compensated systems, i.e., for smaller Mn concentrations. This indicates the instability of the ferromagnetic state with increasing antisite concentration [see also Fig. 11(b)]. The kink in the dependence of $\bar{J}_1^{Mn,Mn}$ for $x=0.02$ and $y=0.01$ marks the change of p-type doping to n-type doping. The decrease of the dominating exchange interactions with Mn concentration is also in agreement with the frozen-magnon calculations in Ref. 19 using a supercell approach. These results are in striking contrast to those of the simple free-electron model: the amplitude of RKKY oscillations is proportional to the size of the Fermi wave vector k_F,[32] which, in turn, is roughly proportional to $x^{1/3}$. The modified expression for the RKKY interaction in DMS which phenomenologically takes into account the effect of disorder was presented in Ref. 33. In there an exponentially damped factor due to de Gennes[30] was added neglecting, however, the concentration dependence. It should be noted that the amplitude of oscillations has to be regarded as an asymptotic property and conclusions made from its preasymptotic behavior have to be taken with care.

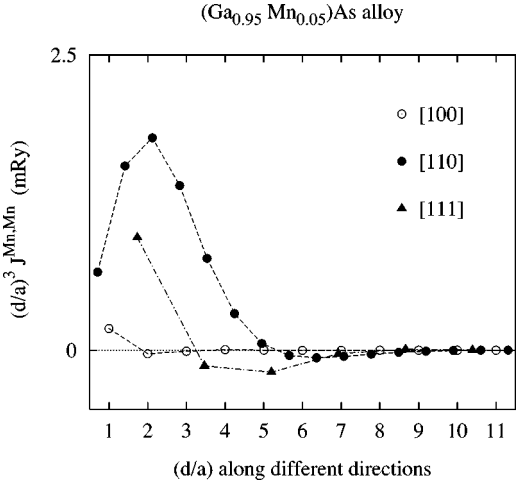

FIG. 6. Exchange interactions $(d/a)^3\bar{J}^{Mn,Mn}(d/a)$ in ferromagnetic $(Ga_{0.95}Mn_{0.05})As$ calculated as a function of the distance d between two Mn atoms along [100], [110], and [111] directions.

In Fig. 6 we show the dependence of the $\bar{J}_{ij}^{Mn,Mn}$ (multiplied by the RKKY prefactor d^3) with respect to the distance d along the directions [100], [110], and [111] in the Ga sublattice of $(Ga_{0.95}Mn_{0.05})As$ alloy. The dominating character of the exchange interactions along the [110] direction can clearly be seen as well as the smallness of the interactions along the [100] direction. The anisotropic character of the exchange interactions, i.e., the Fermi-surface anisotropy along different directions in the BZ, whose spanning vectors determine the periods of the damped oscillations, is also obvious.

It is interesting to compare the behavior of the exchange interactions in $(Ga_{0.95}Mn_{0.05})As$ and $(Ga_{0.95}Mn_{0.05})N$ alloys. The GaN-based DMS behave quite differently as compared to conventional GaAs-based DMS,[29] namely, (i) the gap in the host GaN semiconductor is significantly larger than that

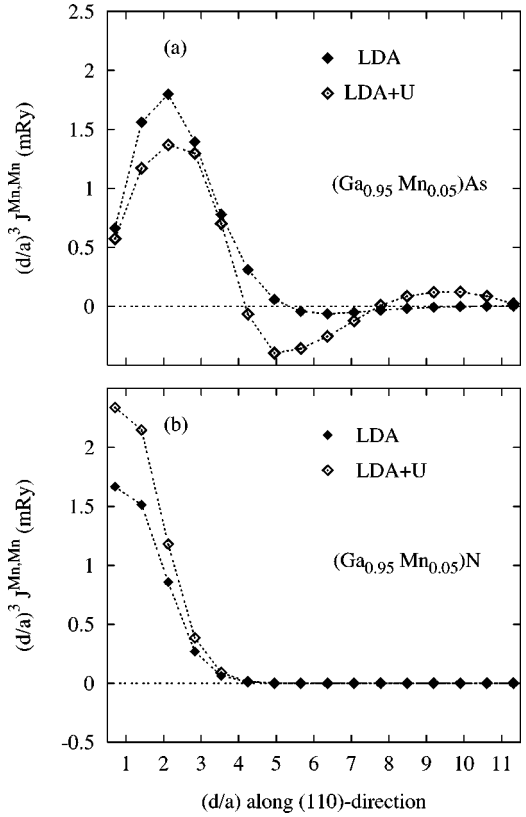

FIG. 7. Exchange interactions $(d/a)^3\overline{J}^{\mathrm{Mn,Mn}}(d/a)$ as a function of the distance d between two Mn atoms evaluated along the nearest-neighbor direction [110] in the LDA and LDA+U: (a) ferromagnetic $(Ga_{0.95}Mn_{0.05})As$ and (b) ferromagnetic $(Ga_{0.95}Mn_{0.05})N$.

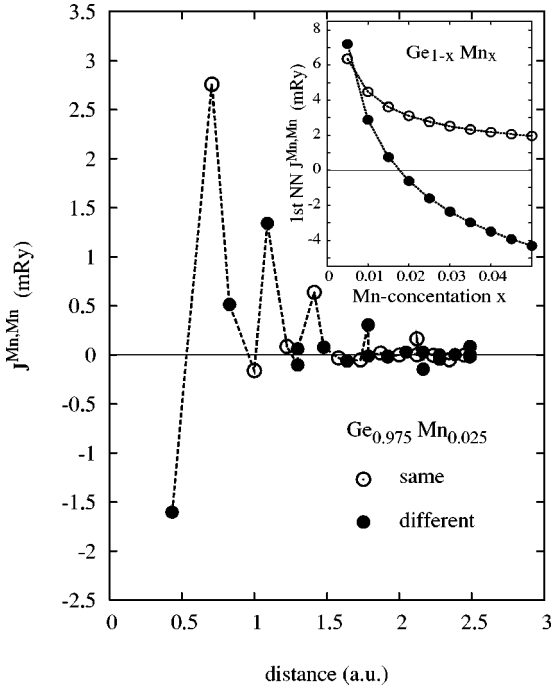

FIG. 8. Exchange pair interactions $\overline{J}_{ij}^{\mathrm{Mn,Mn}}$ for ferromagnetic $Ge_{0.975}Mn_{0.025}$ as a function of distance between Mn impurities. The dependence of the nearest-neighbor exchange interactions $\overline{J}_1^{\mathrm{Mn,Mn}}$ on the Mn concentration is shown in the inset. Empty symbols denote case when sites i and j are on the same sublattice while full symbols refer to sites on different sublattices.

in GaAs, and (ii) the formation of the impurity band of Mn atoms in the gap is due to strong alloy scattering on the Mn atoms. We have also studied the effect of electron correlations for the Mn atoms in the framework of the LDA+U approach, where LDA stands for local-density approximation. The first such study was done by adopting a supercell approach[34] while the present calculations were performed in the framework of the CPA. We have used the same parameters for the correlation energy U (0.3 Ry) and the intrasite exchange energy J (0.08 Ry) as in Ref. 34. The results of both approaches for (Ga,Mn)As alloys agree well: the DOS in the LDA+U is sharper, located further off the Fermi energy, thus leading to an enhanced local moment of the Mn atoms ($3.7\mu_B$ and $4.4\mu_B$ in the LDA and LDA+U, respectively).

Here we shall concentrate on the effect of electron correlations on the exchange interactions in (Ga,Mn)As and (Ga,Mn)N alloys. The results for the dependence of $\overline{J}_{ij}^{\mathrm{Mn,Mn}}$ on the distance d between two Mn atoms (multiplied by the RKKY prefactor d^3) are summarized in Fig. 7. We clearly observe a much stronger damping of the exchange interactions with distance in (Ga,Mn)N which is due to the larger gap in GaN semiconductor and the strong alloy scattering in the impurity band combined with a half-metallic character of the (Ga,Mn)N alloy. Electron correlations slightly enhance exchange interactions which, however, remain well localized in the real space. The damping of the oscillations of $\overline{J}_{ij}^{\mathrm{Mn,Mn}}$ with distance in (Ga,Mn)As alloys is smaller in the LDA+U description than in the LDA. The reason is the above-mentioned downward shift of the Mn levels which reduces the effect of disorder in this energy region and leads to more pronounced oscillations of $\overline{J}_{ij}^{\mathrm{Mn,Mn}}$ with distance [Fig. 7(a)]. For the same reason, the Fermi-surface geometry is changed leading thus to a different period of damped oscillations.

D. $Ge_{1-x}Mn_x$ alloys

The dependence of exchange interactions $\overline{J}_{ij}^{\mathrm{Mn,Mn}}$ on the distance between Mn atoms as well as on their concentration in $Ge_{1-x}Mn_x$ alloys is shown in Fig. 8. In (Ge,Mn) alloys there are two types of exchange interactions, namely, for Mn atoms on the same Ge-sublattice and on different Ge sublattices. With the exception of the nearest neighbor (NN) $\overline{J}_{ij}^{\mathrm{Mn,Mn}}$ between Mn atoms on different Ge sublattices, the dominating interactions for $Ge_{0.975}Mn_{0.025}$ are ferromagnetic. It should be pointed out that the present calculations exhibit a strong concentration dependence of $\overline{J}_{ij}^{\mathrm{Mn,Mn}}$ as can be seen from the inset of Fig. 8 for the first NN terms between Mn atoms on the same and different Ge sublattices. We see that for larger Mn concentrations we have antiferromagnetic coupling between nearest-neighbor Mn atoms on different sublattices which in turn is in qualitative agreement with the results of Ref. 4. However, for smaller Mn concentrations, the antiferromagnetic character of the $\overline{J}_1^{\mathrm{Mn,Mn}}$ on different

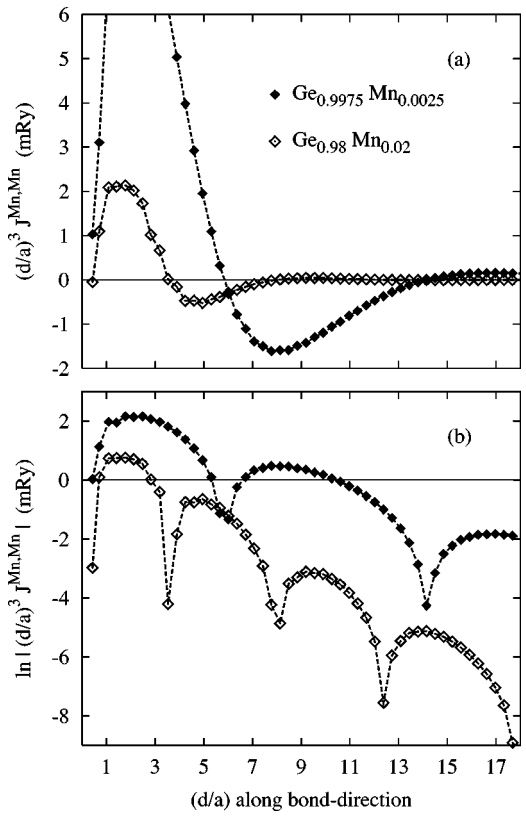

FIG. 9. Exchange interactions between pairs of Mn impurities in $Ge_{0.9975}Mn_{0.0025}$ (full symbols) and $Ge_{0.98}Mn_{0.02}$ (empty symbols) as a function of the distance $d=|\mathbf{R}_i-\mathbf{R}_j|$ along the bond direction: (a) $(d/a)^3\overline{J}_{ij}^{\mathrm{Mn,Mn}}(d/a)$ and (b) $\ln|(d/a)^3\overline{J}_{ij}^{\mathrm{Mn,Mn}}(d/a)|$.

sublattices is reduced and the coupling becomes ferromagnetic for $x<0.015$. On the other hand, the $\overline{J}_1^{\mathrm{Mn,Mn}}$ between Mn atoms on the same Ge sublattices decrease with increasing x but remain ferromagnetic, and a pronounced concentration dependence is found only for small Mn concentrations. This behavior is quite similar to that of the $\overline{J}_1^{\mathrm{Mn,Mn}}$ in (Ga,Mn)As [see the inset in Fig. 5(a), case $y=0.0$]. It is obvious from Fig. 8 and Eq. (4) that the $\overline{J}_{ij}^{\mathrm{Mn,Mn}}$ for more distant pairs of Mn atoms influence the value of T_c significantly as is the case in GaAs-based DMS.

In Fig. 9 we present the exchange interactions $\overline{J}^{\mathrm{Mn,Mn}}$ multiplied by the RKKY prefactor d^3, Fig. 9(a), as well as in Fig. 9(b) in the form $\ln|d^3\overline{J}_{ij}^{\mathrm{Mn,Mn}}|$, along the bond direction (d is the distance between Mn pairs). The following conclusions can be made:

(i) Substitutional disorder and the nearly half-metallic character of (Ge,Mn) alloys lead to a strong, exponential damping of the RKKY-type oscillations. The exponential character of the damping of oscillations is clearly seen from Fig. 9(b).

(ii) In accordance with a RKKY-type picture the period of the damped oscillations is inverse proportional to the size of the hole Fermi surface, i.e., to the concentration of Mn impurities.

(iii) As to expected, the exponential damping [the slope of curves in Fig. 9(b)] increases with the concentration x because disorder in the system increases with the Mn concentration. The damping is, however, smaller than in (Ga,Mn)As alloys with the same concentration of Mn impurities.

(iv) The ferromagnetic character of the exchange interactions is preserved even for distances larger as compared to the average distance between two Mn impurities.

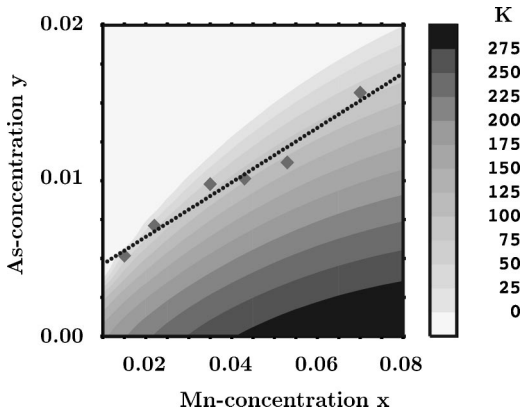

FIG. 10. Contour plot of the Curie temperature of ferromagnetic $(Ga_{1-x-y}Mn_xAs_y)As$ as a function of the composition (x,y). The diamonds refer to experimental values (Ref. 1) (see the text), the dotted line represents a least-square fit to these data.

E. Curie temperatures: $(Ga_{1-x-y}Mn_xAs_y)As$ and $Ge_{1-x}Mn_x$

The general trend of Curie temperatures in $(Ga_{1-x-y}Mn_xAs_y)As$ is illustrated in Fig. 10 as a function of the chemical composition (x,y). T_c increases with x in systems without As antisites and reaches the room temperature at approximately $x=0.05$. Detailed results for $(Ga_{1-x-y}Mn_xAs_y)As$ alloys without $(y=0.0)$ and with $(y=0.01)$ As antisites are presented in Fig. 11(a). In both cases T_c saturates for higher Mn concentrations and then decreases. Such a behavior is the result of the interplay between two effects, namely, a decrease of the exchange interactions with respect to the Mn concentration [see the inset in Fig. 5(a)] which reduces T_c, and the factor x in the expression (4) which increases T_c. The same trend and similar values of T_c were also obtained recently in the framework of the CPA approach[29] and a frozen-magnon approach using large ordered supercells.[19] The Curie temperature for a fixed Mn concentration is strongly reduced with increasing concentration of As antisites. This result which is known also from model studies[2,3] clearly indicates a strong correlation between T_c and the number of carriers. It should be noted that the number of carriers is used in model studies only as an empirical parameter. For $y=0.01$ T_c is reduced by $\approx 100-150$ K over the whole range of Mn concentrations as compared to the case of $y=0.0$. This is in fair agreement with the experimental data for ferromagnetic metallic samples $(0.035<x<0.055)$.[1]

The concentration of As antisites y in Mn enriched samples is not well known from the experiment.[1] A detailed knowledge of T_c as a function of x and y as shown in Fig. 10 allows us to estimate the relation between x and y in such systems. In Fig. 10 we have inserted the experimental points

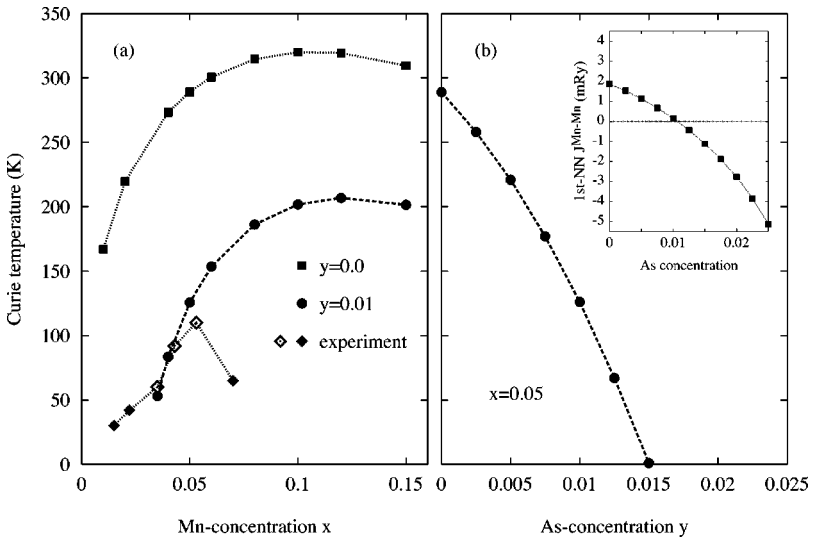

FIG. 11. (a) Curie temperatures of $(Ga_{1-x-y}Mn_xAs_y)As$ in the ferromagnetic state, Eq. (6), as a function of x for $y=0$ and $y=0.01$ as compared to the experiment, Ref. 1 (empty diamonds: metallic ferromagnet, full diamonds: nonmetallic samples); (b) Curie temperatures of ferromagnetic $(Ga_{0.95-y}Mn_{0.05}As_y)As$ as a function of y. The dependence of the nearest-neighbor exchange interactions $\overline{J}_1^{\mathrm{Mn,Mn}}$ on the concentration of As antisites for a fixed Mn concentration $x=0.05$ is shown in the inset.

for each experimental T_c that corresponds to a given x and determined the concentration y such that the calculated and experimental[1] T_c coincide. The data obtained in this way follow approximately a straight line, which in turn suggests that the number of As antisites increases with the concentration of Mn atoms. A recent evaluation of formation energies of the As-antisite defects in (Ga,Mn)As (Ref. 35) confirms this conclusion.

For a fixed Mn concentration the dependence of T_c on the concentration of As antisites is presented in Fig. 11(b), and shows a monotonic decrease of T_c with increasing y due to the decreasing number of holes in the valence band which in turn mediates the ferromagnetic coupling between Mn atoms. This result is in qualitative agreement with predictions of the KEM model.[2,3] As to be expected, the leading $\overline{J}_1^{\mathrm{Mn,Mn}}$ depend on the Mn concentration in the same manner as the Curie temperature [see inset in Fig. 11(b)]. $\overline{J}_1^{\mathrm{Mn,Mn}}$ becomes antiferromagnetic for a slightly smaller x than the value at which T_c disappears. This again confirms the fact that next nearest neighbors $\overline{J}^{\mathrm{Mn,Mn}}$ are also important for the Curie temperature.

The calculated mean-field values of T_c, Eq. (6), for $Ge_{1-x}Mn_x$ alloys as a function of concentrations are presented in Fig. 12 together with available experimental data.[4] The present results are also compared with the percolation model calculations of Ref. 4. The calculated mean-field values of T_c for $Ge_{1-x}Mn_x$ alloys are in fair qualitative agreement with the experiment, which similar to (Ga,Mn)As alloys also show a monotonic increase of T_c with the concentration x and saturation for higher Mn concentrations. The concentration of magnetically active Mn atoms in the experiment is smaller than the actual Mn concentration x.[4] Assuming a total magnetic moment per Mn atom close to $3\mu_B$, the authors of Ref. 4 estimate that only about 40–60 % of Mn atoms are magnetically active. This was approximately taken into account here by assuming that $x_{eff}=x/2$, where x_{eff} is the effective Mn concentration. The results shown in Fig. 12 are in better agreement with the experiment but still overestimate T_c. This deviation can be caused by (i) Mn atoms being in the interstitial rather than in the substitutional position; (ii) the fact that MFA usually overestimates T_c; and (iii) possible clustering of Mn atoms and other local environment effects, which are neglected in the present MFA study. The latter two effects can be accounted for in the framework of the Monte Carlo simulation in terms of an effective Heisenberg model. It should be noted that the present results are in better agreement with the experiment than the percolation model of Ref. 4.

F. Effect of disorder on Curie temperature

The damping of the exchange interactions due to disorder and the half-metallic character of the DMS is usually neglected in model studies. In a supercell approach, the half-metallic character of the system under investigation is in-

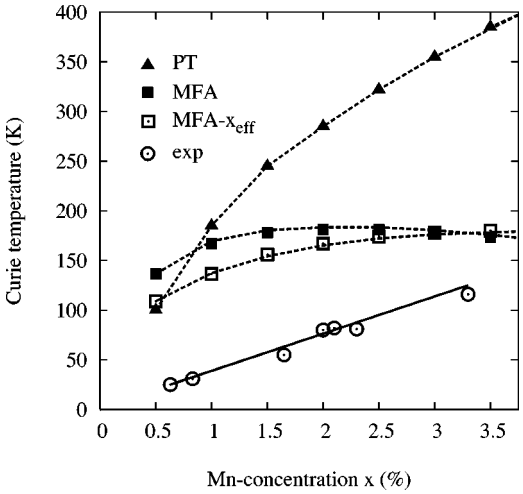

FIG. 12. Curie temperatures of $Ge_{100-x}Mn_x$ alloys as a function of the concentration of Mn atoms: experimental values for (Ge,Mn) alloys (exp, Ref. 4); the mean-field values determined from Eq. (6) (MFA, full squares); the results of the percolation theory (PT) for (Ge,Mn) alloys in Ref. 4 (triangles). Also shown are the mean-field values determined for the effective Mn concentration $x_{eff}=x/2$ (open squares, see the text).

cluded while the effect of disorder due to impurities is neglected. In the following we illustrate the effect of impurities on T_c by comparing fully *ab initio* calculations based on the CPA with simplified models.

In the first model we assume that in $(Ga_{0.95}Mn_{0.05})As$ the number of holes n_h in the valence band corresponds to that in $(Ga_{0.95-y}Mn_{0.05}As_y)As$, i.e., $n_h = 0.05 - 2y$. The effect of disorder due to As antisites which represent a strong perturbation of the host electronic structure [see Fig. 1(a)] is thus neglected (the rigid band model). Results for T_c obtained by full and rigid band calculations are $T_c = 221$ K and $T_c = 195$ K for $y = 0.005$, respectively, and 126 and 79 K for $y = 0.01$. While the trend is the same, i.e., a causing reduction of T_c with a reduced number of hole carriers, there are non-negligible quantitative differences when increasing y.

In the second model, we compare T_c for two systems $(Ga_{0.92}Mn_{0.05}As_{0.01}Zn_{0.02})As$ and $(Ga_{0.94}Mn_{0.05}As_{0.01})(As_{0.98}C_{0.02})$, which have the same number of Mn atoms and the same concentration of holes as in the reference $(Ga_{0.95}Mn_{0.05})As$ alloy. In both alloys, Zn dopants on the Ga sublattice and C impurities on the As sublattice act as acceptors by compensating two electrons created in the valence band by each As antisite. Because the numbers of Mn atoms and the hole concentration in the valence band are the same, the KEM predicts the same T_c in both alloys as in the reference case, namely 289 K. Full calculations taking into account the effect of disorder yield for the Zn- and C-doped alloys $T_c = 282$ and 260 K, respectively. This result is easy to understand: Zn impurities influence states lying far below the Fermi energy in the valence band, leaving thus the hole Fermi surface essentially unchanged. On the other hand, C dopants influence also states close to the Fermi energy, leading thus to a larger deviation from the reference value.

IV. CONCLUSIONS

We have performed self-consistent electronic structure calculations for DMS within the local-density approximation by treating disorder within the framework of the coherent-potential approximation. Based on these first-principles calculations we have determined effective pair exchange interactions for (Ga,Mn)As and (Ge,Mn) alloys and presented a detailed study of their dependence on the distance between the Mn atoms as well as on their concentration and compensating defects. As a simple utilization of the calculated exchange interactions we present a mean-field study of Curie temperatures.

The main results can be summarized as follows:

(i) (Ga,Mn)As and (Ge,Mn) alloys exhibit ferromagnetic behavior with total magnetic moments per Mn atom of $4\mu_B$ and $3\mu_B$, respectively. Both systems exhibit half-metallic behavior with filled minority subbands.

(ii) In both systems the exchange interactions between the Mn atoms are ferromagnetic for distances larger than the average nearest Mn Mn distance as assumed in model studies.

(iii) In both alloys the calculated exchange interactions exhibit oscillatory character and are exponentially damped by disorder and due to the half-metallic character of minority bands, whereas the isolated Mn impurities in the semiconductor host with the same number of valence holes exhibit an undamped RKKY-type behavior. The period of the damped oscillations is inversely proportional to the number of valence holes (concentration of Mn atoms).

(iv) The presence of compensating defects such as, e.g., As antisites in (Ga,Mn)As which reduce the number of holes in the valence band, leads to a longer period of damped oscillations.

(v) The exchange interactions between Mn atoms in (Ga,Mn)As are reduced with increasing concentrations of both Mn and As impurities. The first nearest-neighbor interactions between Mn atoms are ferromagnetic but become antiferromagnetic in highly compensated systems.

(vi) The nearest-neighbor exchange pair interactions $\overline{J}_1^{\mathrm{Mn,Mn}}$ in (Ge,Mn) alloys decrease with increasing Mn concentration but remain ferromagnetic for Mn pairs on the same Ge sublattices while for Mn pairs on different sublattices they become antiferromagnetic with increasing Mn concentration.

(vii) The Curie temperature for (Ga,Mn)As alloys is strongly reduced by increasing the concentration of As antisites. A comparison of the calculated and the measured concentration dependences of the Curie temperature indicates a correlation between the concentration of Mn impurities and of As antisites, namely, an increase of the donor concentration with an increase of the Mn content.

(viii) The Curie temperature for (Ge,Mn) alloys increases monotonically with the Mn concentration.

ACKNOWLEDGMENTS

The research was carried out within the Project No. AVOZ1-010-914 of the Academy of Sciences of the Czech Republic and was supported by the Grant Agency of the Academy of Sciences of the Czech Republic (Grant No. A1010203), the CMS Vienna (Grant No. GZ 45.504), and the RTN *Computational Magnetoelectronics of EU* (Grant No. HPRN-CT-2000-00143). We acknowledge discussions with B. Jonker concerning GeMn alloys.

[1] H. Ohno, J. Magn. Magn. Mater. **200**, 110 (1999).

[2] K. König, J. Schliemann, T. Jungwirth, and A.H. MacDonald, in *Electronic Structure and Magnetism in Complex Materials*, edited by D.J. Singh and D.A. Papaconstantopoulos (Springer-Verlag, Berlin, 2003).

[3] T. Dietl, H. Ohno, and F. Matsukura, Phys. Rev. B **63**, 195205 (2001).

[4] Y.D. Park, A.T. Hanbicki, S.C. Erwin, C.S. Hellberg, J.M. Sullivan, J.E. Mattson, T.F. Ambrose, A. Wilson, G. Spanos, and B.T. Jonker, Science **295**, 651 (2002).

[5] S. Cho, S. Choi, S.C. Hong, Yu. Kim, J.B. Ketterson, B.-J. Kim, Y.C. Kim, and J.-H. Jung, Phys. Rev. B **66**, 033303 (2002).
[6] A.I. Liechtenstein, M.I. Katsnelson, V.P. Antropov, and V.A. Gubanov, J. Magn. Magn. Mater. **67**, 65 (1987).
[7] M. Pajda, J. Kudrnovský, I. Turek, V. Drchal, and P. Bruno, Phys. Rev. B **64**, 174402 (2001).
[8] I. Turek, J. Kudrnovský, G. Bihlmayer, and S. Blügel, J. Phys.: Condens. Matter **15**, 2771 (2003); I. Turek, J. Kudrnovský, M. Diviš, P. Franek, G. Bihlmayer, and S. Blügel, Phys. Rev. B **68**, 224431 (2003).
[9] M. Pajda, J. Kudrnovský, I. Turek, V. Drchal, and P. Bruno, Phys. Rev. Lett. **85**, 5424 (2000).
[10] S. Sanvito, P. Ordejón, and N.A. Hill, Phys. Rev. B **63**, 165206 (2001).
[11] M. van Schilfgaarde and O.N. Mryasov, Phys. Rev. B **63**, 233205 (2001).
[12] M. Jain, L. Kronik, J.R. Chelikowsky, and V.V. Goglevsky, Phys. Rev. B **64**, 245205 (2001).
[13] E. Kulatov, H. Nakayama, H. Meriette, H. Ohta, and Yu.A. Uspenskii, Phys. Rev. B **66**, 045203 (2002).
[14] F. Máca and J. Mašek, Phys. Rev. B **65**, 235209 (2002).
[15] H. Akai, Phys. Rev. Lett. **81**, 3002 (1998).
[16] K. Sato and H. Katayama-Yoshida, Jpn. J. Appl. Phys., Part 2 **40**, L651 (2001).
[17] T.C. Schulthess and W.H. Butler, J. Appl. Phys. **89**, 7021 (2001).
[18] P.A. Korzhavyi, I.A. Abrikosov, E.A. Smirnova, L. Bergqvist, P. Mohn, R. Mathieu, P. Svedlindh, J. Sadowski, E.I. Isaev, Yu.Kh. Vekilov, and O. Eriksson, Phys. Rev. Lett. **88**, 187202 (2002).
[19] L.M. Sandratskii and P. Bruno, Phys. Rev. B **66**, 134435 (2002).
[20] O.K. Andersen and O. Jepsen, Phys. Rev. Lett. **53**, 2571 (1984).
[21] S.H. Vosko, L. Wilk, and M. Nusair, Can. J. Phys. **58**, 1200 (1980).
[22] I. Turek, V. Drchal, J. Kudrnovský, M. Šob, and P. Weinberger, *Electronic Structure of Disordered Alloys, Surfaces and Interfaces* (Kluwer, Boston, 1997); I. Turek, J. Kudrnovský, and V. Drchal, in *Electronic Structure and Physical Properties of Solids*, edited by H. Dreyssé, Lecture Notes in Physics Vol. 535 (Springer, Berlin, 2000), pp. 349–378.
[23] P. Bruno, J. Kudrnovský, V. Drchal, and I. Turek, Phys. Rev. Lett. **76**, 4254 (1996).
[24] J. Kudrnovský, V. Drchal, I. Turek, P. Bruno, and P. Weinberger, in *Electronic Structure and Physical Properties of Solids*, edited by H. Dreyssé, Lecture Notes in Physics Vol. 535 (Springer, Berlin, 2000), pp. 313–346.
[25] J.A. Blackman and R.J. Elliott, J. Phys. C **2**, 1670 (1969).
[26] J. König, T. Jungwirth, and A.H. MacDonald, Phys. Rev. B **64**, 184423 (2001).
[27] G. Bouzerar, J. Kudrnovský, L. Bergqvist, and P. Bruno, Phys. Rev. B **68**, 081203 (2003).
[28] J. Kudrnovský, I. Turek, V. Drchal, F. Máca, J. Mašek, P. Weinberger, and P. Bruno, J. Supercond. **16**, 119 (2003).
[29] K. Sato, P.H. Dederichs, and H. Katayama-Yoshida, Europhys. Lett. **61**, 403 (2003).
[30] P.J. de Gennes, J. Phys. Radium **23**, 630 (1962).
[31] P.M. Levy, S. Maekawa, and P. Bruno, Phys. Rev. B **58**, 5588 (1998).
[32] Ch. Kittel, *Quantum Theory of Solids* (Wiley, New York, 1987).
[33] F. Matsukura, H. Ohno, A. Shen, and Y. Sugawara, Phys. Rev. B **57**, R2037 (1998).
[34] J.H. Park, S.F. Kwon, and B.I. Min, Physica B **281&282**, 703 (2000).
[35] J. Mašek, I. Turek, V. Drchal, J. Kudrnovský, and F. Máca, Acta Phys. Pol. A **102**, 673 (2002).